Magnetic configurations in thin films with competing interactions

Author: Víctor Barrera Consuegra
Dpt. Física de la Matèria Condensada, Facultat de Física,
Universitat de Barcelona, Av. Diagonal 645, 08028 Barcelona, Spain.

Advisor: Òscar Iglesias Clotas

Abstract: In this work, the ground state configurations of magnetic thin films and some finite size magnetic elements are studied by means of Monte Carlo simulations. For this purpose, we have set up a code to simulate Ising and Heisenberg spin classical models on squared and triangular lattices including exchange (J), dipolar (g) interactions and magnetocrystalline anisotropy (K). We show how the interplay between short and long-ranged interactions stabilizes stripe-like patterns similar to those observed experimentally. Phase diagrams in the (J/g, T) and (K/g, T) planes are presented and the corresponding reorientation transitions are characterized, stressing the differences when comparing different lattices. Finally, the magnetic configurations obtained for thin films are compared to those for systems of finite-size, demonstrating that our code can be used also to study the properties of nanoscale elements.

I. INTRODUCTION

Magnetic thin films and quasi two dimensional materials have been extensively studied in the last decades because of their use in technological applications such as magnetic recording and sensing or spintronics[1] that has been driven by the need to decrease the typical size of devices to the nanometric scale[2]. The ability to prepare continuous films with well defined atomic structure deposited on non-magnetic substrates allows to tune the stable magnetic state from parallel to perpendicular to the film surface by changing the thickness and materials composition. Different microscopy and structural characterization techniques have helped to understand the interplay between transport and magnetic properties, evidencing the existence of non-uniform magnetic patterns with striped or bubble-like shapes .

From a theoretical point of view, it has been acknowledged that the formation of such domain structures requires the competition between short and long-ranged interactions[3,4]. The presence of perpendicular magnetic anisotropy further enriches the possibilities as it competes with the main demagnetizing character of the magnetostatic interactions. While this kind of systems have been studied with some detail in the past, there are still open and controversial points that need to be clarified for certain regions of the main parameters (J, g, K)[5]. In this work, we will perform simulations of a model of a thin film with the aim to study the variety of ground state configurations that can be attained, to establish phase diagrams for their stability, and to investigate possible reorientation transitions (RT) of the magnetization. The work is an extension of preliminary results obtained in Ref. 6 for small sizes and using a cut-off for the dipolar interactions, which may introduce spurious effects. For this purpose, we have set up a new code with improved capabilities that will allow us to ascertain some of the speculative results presented there and to explore cases not previously considered.

II. MODEL AND SIMULATION DETAILS

In our model Hamiltonian for a thin film, we will treat atomic magnetic moments as classical vector (Heisenberg) spins of unit magnitude represented by the variables $\vec{S}_i$ at the nodes of a 2D regular lattice which can be either squared or triangular with a total number of spins $N = L \times L$. Three individual contributions to the energy will be considered: exchange and dipolar interactions, and magnetocrystalline anisotropy. The relative contribution of each term is characterized by three constants g, J and K that include the dependence on the lattice parameter and the magnetic moment of the spins. They can be factored out from their respective expressions, resulting in a total interaction energy:

$$E = JE_{ex} + gE_{dip} + KE_{ani} \ . \tag{1}$$

Indeed, we will fix $g = 1$ in what follows and study the behaviour of our system in term of rescaled parameters J/g and K/g.

The exchange interaction acts at an atomistic level and it has short-range character. The corresponding energy can be written as:

$$E_{ex} = -\sum_{<i,j>} \vec{S}_i \cdot \vec{S}_j, \tag{2}$$

where the sum extends to nearest neighbours (nn). We will focus here in ferromagnetic (FM) materials for which $J \geq 0$, which favour parallel orientation of neigbouring spins.

The dipolar interaction is long-ranged and acts between atomistic or macroscopic magnetic moments, and is responsible for the formation of magnetic domains. It can be written as:

$$E_{dip} = \sum_{i \neq j}^{N} \left(\frac{\vec{S}_i \cdot \vec{S}_j}{r_{ij}^3} - 3\frac{(\vec{S}_i \cdot \vec{r}_{ij})(\vec{r}_{ij} \cdot \vec{S}_j)}{r_{ij}^5} \right) \ , \tag{3}$$

where $\vec{r}_{ij}$ is the vector connecting spins i and j. The first term produces an antiferromagnetic (AF) order, while the second term acts essentially as an effective in-plane anisotropy. In order to decouple the spin and spacial dependencies of E_{dip}, it is convenient to introduce the set of dipolar matrices $W_{nm}^{\alpha\beta}$

$$W_{ij}^{\alpha\beta} = \frac{1}{r_{ij}^3}\left(\delta_{\alpha\beta} - \frac{3\delta_{\alpha\gamma}\delta_{\beta\eta}r_{ij}^{\gamma}r_{ij}^{\eta}}{r_{ij}^2}\right) . \tag{4}$$

They have dimension $N \times N$ and their elements depend only on the positions of the spins in the lattice, not on their orientations. They can be calculated once at the beginning of the program and stored in memory for latter use. Here i, j label each interacting spin couple, while $\alpha, \beta = 1, 2, 3$ refer to cartesian components. Having these matrices, the dipolar field acting on spin $\vec{S}_i$ can be defined in components as

$$(h_{dip})_i^{\alpha} = \sum_{i \neq j}\sum_{\beta} W_{ij}^{\alpha\beta} S_j^{\beta} , \tag{5}$$

and the energy can be simply computed as

$$E_{dip} = \sum_{i}^{N} \vec{S}_i \cdot \vec{h}_{dip,i} . \tag{6}$$

Finally, we include the on-site magnetic anisotropy, which for a thin film favours alignment of the magnetization along the direction perpendicular to its surface, here the z axis:

$$E_{ani} = -\sum_{i}^{N}(\vec{S}_i \cdot \hat{n})^2 = -\sum_{i}^{N}(S_i^z)^2 . \tag{7}$$

In what follows, we specify some of the details regarding the simulation procedure. Preliminary simulations were run for small system sizes ($L = 16$) in order to determine the main parameter regions that stabilize the different magnetic configurations. Refined calculations have been performed on lattices of size $L = 32$ in order to capture details at some regions of the phase diagrams. A single code allows to choose between Heisenberg and Ising spins, to choose squared or triangular lattices and to decide if periodic boundary (PB) conditions have to be implemented. After the geometry and spin configuration is settled, a list of nn and the dipolar matrices are computed and stored in memory. The code implements the well-known Monte Carlo (MC) method with the Metropolis algorithm for continuous spins.

The MC simulations are started from a high temperature with a disordered initial configuration and its energy, exchange and dipolar fields are computed. The energy changes can be easily calculated knowing the values of the stored exchange and dipolar fields and, if a new spin direction is accepted by the Metropolis algorithm, all three quantities are updated based on the energy and spin changes, achieving optimization of the code by an order of magnitude in CPU time. To compute thermodynamic averages, we decrease the temperature (T) in constant steps, while to study ground state configurations we implement a simulated annealing protocol down to $T \approx 0.01$. At every T a minimum of 4000 MC steps were used for thermalisation and 8000 more to calculate averages of the relevant quantities such as energy, magnetization, specific heat and order parameters discussed later on. To prevent finite size effects PB conditions are implemented. These have to be carefully treated for the dipolar interactions by introducing a sufficiently large number of replicas (see Ref.6 for the details).

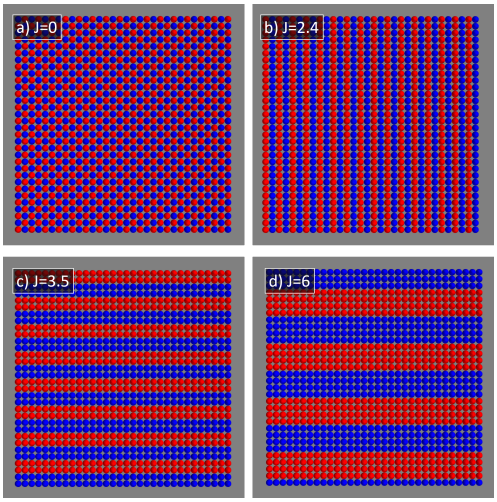

FIG. 1: Ground state configurations found for $J = 0, 2.4, 3.5, 6$ in a 32×32 Ising SC lattice, showing AF order and striped domains of widths $1, 2, 4$. Different colours represent opposite orientations along the direction perpendicular to the film plane.

III. SQUARE LATTICE RESULTS

In this section, we consider the simple cubic geometry in two dimensions (SC) in which every spin has 4 nn and no frustration effects are expected. This case have been thoroughly studied in the past by several groups[5,7,8] although a complete understanding for all the range of parameters is still lacking. Some of these results will be used here as a benchmark for the software we developed.

Ising Model. We start by considering the case of Ising spins pointing perpendicular to the film plane, that can be considered as the $K = +\infty$ limit of the model 1. We have scanned a range of J/g values tracking the characteristic values for which different magnetic orders occur at low temperatures and representative snapshots of the configurations are presented in Fig. 1.

In the absence of exchange interactions, the ground state is the AF Néel checkboard state that can be seen in Fig. 1 (a), that minimizes the dipolar interaction alone. This state persists when introducing the exchange inter-

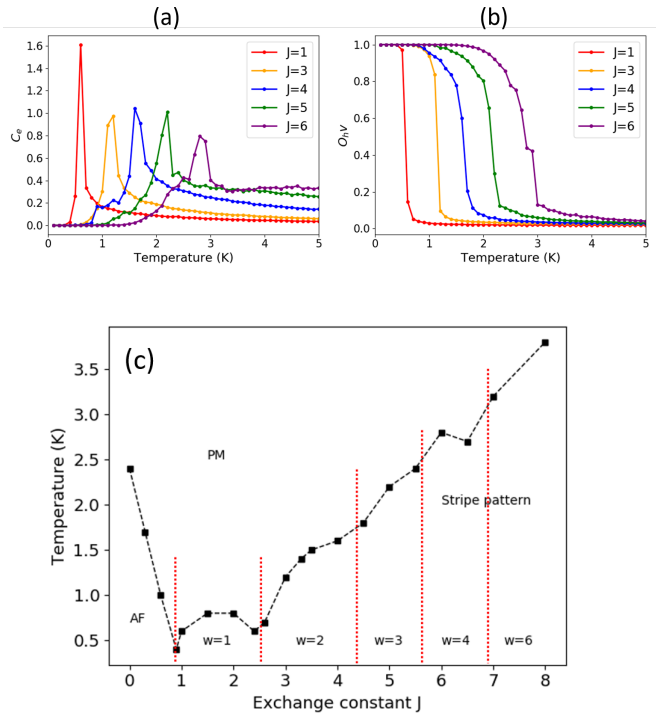

FIG. 2: Thermal dependence of (a) the specific heat and (b) stripe order parameter in a $L = 32$ SC lattice for $J = 1, 3, 4, 5, 6$. (c) The phase diagram for the Ising SC lattice obtained from the maxima in the specific heat, showing between the regions of stability of the AF, PM phases and various stripe phases of width w.

action for J up to $J \simeq 0.88$ due to the dominance of the dipolar AF term of Eq. 3. For increasing values of J, though, the short-range effects of the exchange interaction start to compete with the AF state favoured by g and, consequently, FM stripes of alternating orientation are formed. Their width w increases rapidly with increasing[5] J, as can be seen in the examples shown in Fig. 1 (b-d). Notice that only stripes with w commensurable with the lattice size can be stabilized.

The critical temperatures T_c for the transition between the AF or striped states found in Fig. 2 (c) and the disordered paramagnetic (PM) state, have be determined from the maxima of the thermal dependence of the specific heat shown in Fig. 2 (a) for selected values of J. As has been previously noted[7], this transitions are of first order for small J as signalled by the sharp peak in $C_e(T)$ and become smeared for the wider striped phases, indicating a change to a continuous transition. This fact is corroborated by the thermal dependence of the stripe order parameter shown in Fig. 2 (b), defined as

$$O_{hv} = \left\langle \frac{|n_h - n_v|}{n_h + n_v} \right\rangle , \qquad (8)$$

where $n_{h,v}$ count the number of horizontal/vertical nn antiparallel pairs. Tracking the dependence of T_c on J, we were able to construct the phase diagram (J/g vs T) shown in Fig. 2, where we have also delineated with vertical dashed lines the transitions between striped phases from exact calculations[7]. These transitions have been corroborated by our simulations up to the phase with $w = 8$ although the limits for wide stripes become diffuse due to our limited lattice size. We notice that T_c decreases linearly with J in the AF phase, while it increases in a non-monotonous way for the striped phases.

Heisenberg Model. Now we introduce our results for the Heisenberg model, for which spins can point in any direction. The aim here is to examine the how the competition between the dipolar interaction and anisotropy can induce a RT from in-plane to out-of-plane configurations as K increases, considering first the pure dipolar case with $J = 0$ and considering later the effect of exchange.

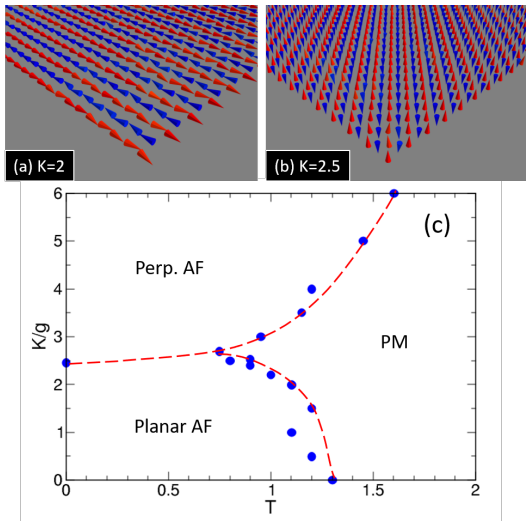

FIG. 3: Upper panels show snapshots of configurations found in a $L = 32$ Heisenberg SC lattice with $J = 0$ (dipolar only case) showing the transition from an (a) in-plane ground state for $K = 2$ to (b) an out-of-plane state for $K = 2.5$. Panel (c) shows the phase diagram $(K/g, T)$ for $L = 16$, signalling the stability regions for the states displayed in the panels above.

Simulations of the model with $J = 0$ have allowed us to identify the occurrence of two kind of states shown in Fig. 3 (a,b). For small K the system orders forming in-plane FM columns with AF order between them. This configuration minimizes the dipolar interaction along both spatial directions in SC lattice and is stable up to $K \simeq 2.46$[8]. For higher K, a transition to a check-board AF state with out-of-plane order is stabilized similar to the one shown in Fig. 1 (a) for the Ising model. Simulations sweeping a range of K values have allowed us to establish the approximate phase diagram shown in Fig. 3 (c).

Next, we introduce the exchange interaction into the model, showing results for a system with $J/g = 1$, which for the Ising case displayed $w = 1$ stripes in the ground state. The resulting phase diagram is displayed in Fig. 4(a). Unlike the previous ($J = 0$) case, for small K, the in-plane configuration is now a FM state [see Fig.

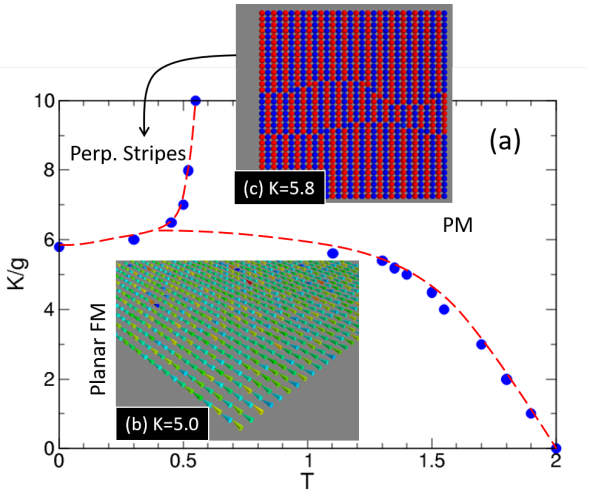

FIG. 4: Snapshots of configurations found in a $L = 32$ Heisenberg SC lattice with $J/g = 1$ ($w = 1$ striped phase) showing the transition from an (a) in-plane ground FM state for $K = 5$ to (b) an out-of-plane state for $K = 5.8$. The colouring scheme corresponds to the projections along the direction perpendicular to the film plane. In (c), we show the corresponding phase diagram in the $(K/g, T)$ plane, where dashed red lines mark the separation between the different magnetic orders.

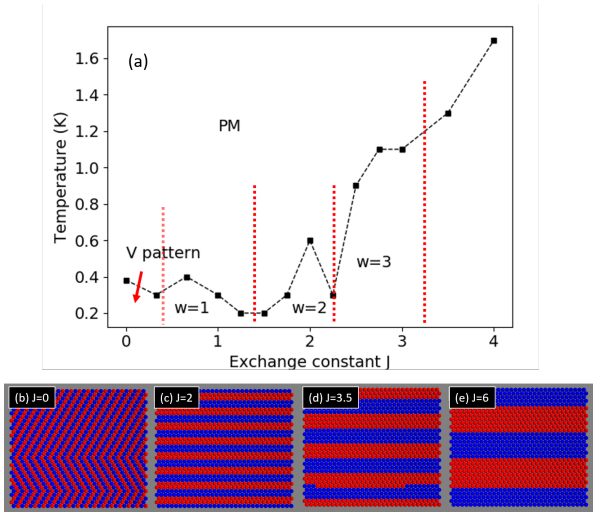

FIG. 5: (a) Phase diagram of the $L = 32$ Ising triangular lattice where the vertical dotted lines mark approximatively the transitions between striped phases of different width w. Panels (b) to (e) show snapshots of the low T configurations for $J = 0, 2, 3.5, 6$.

4(b)] caused by the prevalence of the exchange interaction over the magnetostatic contribution. On the other hand, when increasing K, the system shows a RT towards states with AF stripes perpendicular to the film plane [see Fig. 4(c)] similar to those in Fig.1. The critical value for its occurrence is $K^\star \simeq 5.8$, higher than the value for the pure dipolar case. Notice that the line separating planar from perpendicular states has slightly positive slope. Even so, we have found no evidence of any re-entrance phenomenon with increasing T for $K \simeq K^\star$. The transition from these states is rather abrupt and we have not detected states with canted magnetization for any value of K close to $K^\star$. These probably appear at higher values of J since domain walls may form at the interface between wider stripes[8].

IV. TRIANGULAR LATTICE

Now we repeat the simulations of Sec. III, though using a triangular lattice. One would think that similar results should be obtained, yet in this case a new phenomena needs to be taken into account: magnetic frustration[9]. This phenomenon appears in triangular lattices with AF interactions (whether they are exchange or dipolar). When two neighbouring spins are anti-parallel to each other, a third neighbour cannot satisfy anti-parallel alignment to all the others, hence creating a degenerated ground state.

Ising Model. For an AF Ising model ($g = 0$), the energy would be minimized for any state for which spins in a triangular plaquette are in the 2-up-1 down state, which give rise in particular to striped states that may orient along any of the spatial directions[10]. However, as indicated by the results of our simulations, the dipolar Ising case ($J = 0$) seems to break this degeneracy by selecting diagonal stripes as can be seen in Fig. 5(b), were we see a domain with different orientation that has been formed at $T \neq 0$. This phase is replaced by stripes along the x axis for $J \simeq 0.75$ that, as for the SC lattice, increase in width for increasing J as indicated in the phase diagram and snapshots of Fig. 5(a,c-e). However, in this case, due to frustration induced by the lattice, near the boundaries of the striped phases complicated labyrinthine configurations are obtained. For the same reason, the transitions to the PM phase are more gradual than for the SC lattice and stripes with a given w are stabilized at lower J in the triangular case.

Heisenberg Model. We end this section highlighting some distinctive results for the triangular Heisenberg model. Phase diagrams will not be show due to space limitations, but they resemble qualitatively those obtained for the SC lattice. Now the in-plane ground state for $J = 0$ [shown in Fig. 6 (a)] is FM instead of planar AF and persists up to a value of the anisotropy $K^\star \simeq 3.5$, higher than for the SC lattice. This is also true for the case with $J = 1$, even though now the transition happens for a higher value $K^\star \simeq 7.6$ which is also higher than for the SC lattice. The perpendicular states obtained for $K > K^\star$ are not uniform stripes but complicated labyrinthine domains such as the ones in Fig.6 (d) that are a consequence of frustration. Interestingly, for both cases, we have found states close to the RT that have both in and out-plane magnetization components as can be seen in Figs. 6 (b,c). In the last case, the

configuration seems to have some periodic modulation as also observed in some experiments.

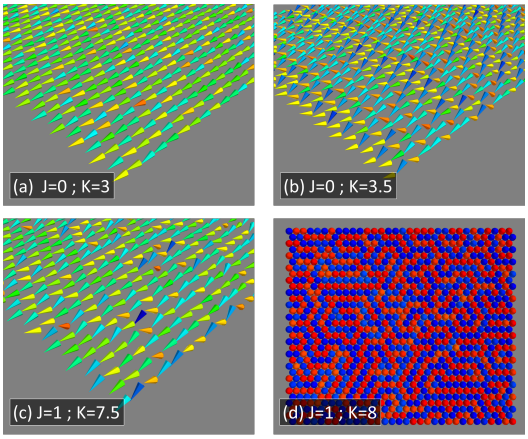

FIG. 6: Snapshots of the low T configurations of a $L = 32$ Heisenberg triangular lattice for K near the RT. Case $J = 0$ for (a) $K = 3$, (b) $K = 3.5$, and case $J = 1$ for (c) $K = 7.5$, (d) $K = 8.0$.

V. FINITE SIZE EFFECTS

All the simulations presented so far have been carried out with PB conditions in order to compare with extensive films. To conclude our study, we would like to show just two examples of ground state calculations of squared nanoelements with free boundary (FB) conditions. We consider for simplicity dipolar lattices with no exchange interaction. As mentioned before in Sec. III, with PB the minimum energy configuration of a planar dipolar assembly is an AF columnar state for the SC lattice while for the triangular lattice it is a planar FM state. However, with FB, these two configurations would create stray fields emanating out of the nanoelement with the consequent cost in dipolar energy. As we can see in Fig. 7, in both cases the dipolar energy is minimized by configurations that close the magnetic flux lines generated by the dipolar fields, with spins parallel to the boundaries of the element and a circulation of the magnetization in the form of vortices.

Interestingly, we observe that the nanoelement shape does not uniquely determine the magnetic pattern, the lattice also matters. Whereas for the SC case [Fig. 7 (a)], displays microvortices which close the dipolar field flux locally, for the triangular lattice [Fig. 7 (b)] a unique vortex extending to the whole element is obtained.

VI. CONCLUSIONS

Using a self-made code, we have performed MC simulations of a thin film with perpendicular anisotropy and competing exchange and dipolar interactions. We have established the existence of different ground state configurations, including striped phases of varying width as well as AF ones for the Ising and Heisenberg models in squared an triangular lattices. The reorientation transition between planar and perpendicular order has been studied and the anisotropy value for its occurrence identified for both lattices. Comparison of configurations obtained for extended films and elements of finite size have also been made and their differences explained. These results can help to understand the origin of the wide variety of magnetic textures observed experimentally in thin films. In future work, we would like to extend the simulations to other values of J/g, to study the role of vacancies and other lattice arrangements in the magnetic order and to study the order of the transitions between the different phases.

Acknowledgments: I would like to thank Dr. Òscar Iglesias for his help, excellent guidance and for his friendly attitude. Also to my former classmates for their overwhelming support, and CSUC for computational resources.

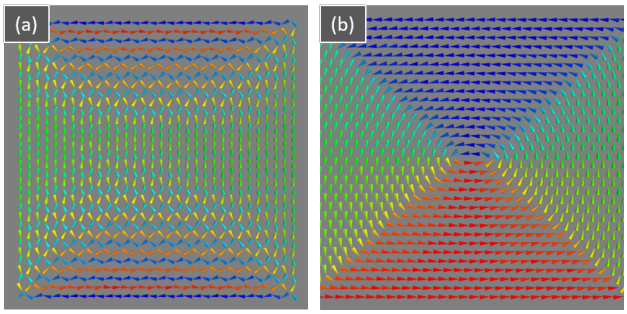

FIG. 7: Ground state configurations after an annealing down to $T = 0.005$ K of $L = 32$ dipolar assemblies with (a) SC and (b) triangular lattice, $J, K = 0$ and $g = 1$.

[1] D. Sander et al., J. Phys. D: Appl. Phys. **50**, 363001 (2017).
[2] S. D. Bader, Rev. Mod. Phys. **78**, 1 (2006).
[3] E. Y. Vedmedenko, *Competing Interactions and Patterns in Nanoworld*, (Wiley-VCH, Weinheim, 2007).
[4] M. Seul, D. Andelman, Science **267**, 476 (1995).
[5] K. De'Bell et al. Rev. Mod. Phys. **72**, 225 (2000).
[6] Òscar Iglesias, *Time dependent processes in magnetic systems*, Ph. D. Thesis, Univ. of Barcelona (2002).
[7] E. Rastelli et al., Phys. Rev. B **76**, 054438 (2007).
[8] M. Carubelli et al., Phys. Rev. B **77**, 134417 (2008); J. P. Whitehead et al., Phys. Rev. B **77**, 174415 (2008).
[9] G.H. Wannier, Phys. Rev. **79**, 357 (1950).
[10] B. A. Ivanov, V. E. Kireev, JETP Lett. **90**, 750 (2009).